

# Low-temperature plasma enhanced atomic layer deposition of large area HfS<sub>2</sub> nanocrystal thin films\*

Ailing Chang(常爱玲)<sup>1</sup>, Yichen Mao(毛亦琛)<sup>1</sup>, Zhiwei Huang(黄志伟)<sup>2</sup>, Haiyang Hong(洪海洋)<sup>1</sup>, Jianfang Xu(徐剑芳)<sup>1</sup>, Wei Huang(黄巍)<sup>1</sup>, Songyan Chen(陈松岩)<sup>1</sup>, and Cheng Li(李成)<sup>1,†</sup>

<sup>1</sup>Department of Physics, OSED, Semiconductor Photonics Research Center, Xiamen University, Xiamen 361005, China

<sup>2</sup>Xiamen University Tan Kah Kee College, Zhangzhou 363105, China

(Received 10 December 2019; revised manuscript received 9 January 2020; accepted manuscript online 16 January 2020)

Hafnium disulfide (HfS<sub>2</sub>) is a promising two-dimensional material for scaling electronic devices due to its higher carrier mobility, in which the combination of two-dimensional materials with traditional semiconductors in the framework of CMOS-compatible technology is necessary. We reported on the deposition of HfS<sub>2</sub> nanocrystals by remote plasma enhanced atomic layer deposition at low temperature using Hf(N(CH<sub>3</sub>)(C<sub>2</sub>H<sub>5</sub>))<sub>4</sub> and H<sub>2</sub>S as the reaction precursors. Self-limiting reaction behavior was observed at the deposition temperatures ranging from 150 °C to 350 °C, and the film thickness increased linearly with the growth cycles. The uniform HfS<sub>2</sub> nanocrystal thin films were obtained with the size of nanocrystal grain up to 27 nm. It was demonstrated that higher deposition temperature could enlarge the grain size and improve the HfS<sub>2</sub> crystallinity, while causing crystallization of the mixed HfO<sub>2</sub> above 450 °C. These results suggested that atomic layer deposition is a low-temperature route to synthesize high quality HfS<sub>2</sub> nanocrystals for electronic device or electrochemical applications.

**Keywords:** HfS<sub>2</sub>, atomic layer deposition, surface morphology

**PACS:** 81.07.Bc, 81.15.Gh

**DOI:** 10.1088/1674-1056/ab6c4a

## 1. Introduction

Two-dimensional (2D) transition metal dichalcogenides (TMDs) are considered as promising candidate materials for optoelectronic devices because of their fascinating electronic, optical, and mechanical properties.<sup>[1–5]</sup> As a member of TMDs family, hafnium disulfide (HfS<sub>2</sub>) is a layered material in which the layers are connected by weak van der Waals forces and Hf and S atoms in the layers are connected by strong chemical bonds. HfS<sub>2</sub> possesses ultrahigh room-temperature carrier mobility, which is necessary for the realization of high-performance electronic devices.<sup>[6]</sup> However, instability of HfS<sub>2</sub> makes it more difficult to synthesis and be applied in atmosphere ambient. Environmental sensitivity study performed on HfS<sub>2</sub> proves that oxidation due to moisture and oxygen adsorption occurs quickly.<sup>[7,8]</sup>

Controllable synthesis of TMDs is necessary for obtaining high quality, uniform, atomic thin films to realize business application. Currently, the synthesis methods of two-dimensional materials are mainly divided into top-down methods (such as mechanical exfoliation and chemical exfoliation) and bottom-up methods (such as chemical vapor deposition and atomic layer deposition).<sup>[4,9]</sup> In current scientific research, most of the 2D TMDs have been obtained by means of mechanical exfoliation, in which single-layer or few layers of HfS<sub>2</sub> are divided by a tape. HfS<sub>2</sub> layers obtained by mechanical exfoliation have high quality, but low yield and poor repeatability, making it difficult to obtain large size films. HfS<sub>2</sub>

films with large size and high uniformity can be achieved by chemical vapor deposition using HfCl<sub>4</sub> powders and sulfur pieces or sulfur powders.<sup>[10–17]</sup> However, the growth temperature of chemical vapor deposition is high, and the quality of the films is greatly affected by the environment inside the reaction chamber.

As a special chemical vapor deposition method, the atomic layer deposition (ALD) has a growth temperature below 500 °C, so it is well compatible with the complementary metal–oxide–semiconductor (CMOS) process. ALD is an indispensable method to combine two-dimensional materials with traditional semiconductors. In addition, ALD has unique self-limiting reaction mechanism, which can grow films with high uniformity, high shape preserving, and precise thickness control. Therefore, ALD has been widely used in the synthesis of 2D TMDs, such as MoS<sub>2</sub>,<sup>[18–26]</sup> WS<sub>2</sub>,<sup>[27–29]</sup> SnS<sub>2</sub>,<sup>[30,31]</sup> and ReS<sub>2</sub>.<sup>[32,33]</sup> So far, HfS<sub>2</sub> and ZrS<sub>2</sub> thin films have been deposited by ALD using HfCl<sub>4</sub> and ZrCl<sub>4</sub> with H<sub>2</sub>S as the precursors.<sup>[34]</sup>

In this work, we synthesized HfS<sub>2</sub> films by remote plasma enhanced atomic layer deposition (RPALD) at lower temperature, with Hf[(C<sub>2</sub>H<sub>5</sub>)(CH<sub>3</sub>)N]<sub>4</sub> (TEMAH) and H<sub>2</sub>S as the reaction precursors. The influence of the deposition temperature on the surface morphology and crystallinity of HfS<sub>2</sub> thin films were analyzed by various characterization techniques. The temperature range of self-limiting reaction behavior and the growth rate were determined. The uniform HfS<sub>2</sub> nanocrystals

\*Project supported by the National Key Research and Development Program of China (Grant No. 2018YFB2200103).

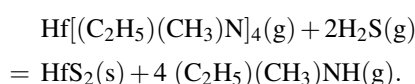
†Corresponding author. E-mail: lich@xmu.edu.cn

were deposited on sapphire, thermally oxidized 300 nm thick silicon dioxide layer (SiO<sub>2</sub>/Si), and silicon (Si) substrates, respectively, and characterized by Raman and x-ray diffraction. The HfS<sub>2</sub> film mixed with hafnium dioxide (HfO<sub>2</sub>) was distinguished, which was easily oxidized under ambient conditions.

## 2. Experimental details

### 2.1. Synthesis of HfS<sub>2</sub> films by RPALD

HfS<sub>2</sub> thin films were deposited in a commercial PRALD setup (R200 Advanced) from PICOSUN. The growth was performed on diverse substrates: sapphire, SiO<sub>2</sub>/Si, and Si. Sapphire and 300 nm SiO<sub>2</sub>/Si substrates were cleaned by acetone, ethanol, and deionized water in an ultrasonic bath for three times. Si was cleaned by boiled H<sub>2</sub>SO<sub>4</sub>/H<sub>2</sub>O<sub>2</sub> (4 : 1) for 10 min, then etched by HF/H<sub>2</sub>O (1 : 20) for 4 min, and washed in deionized water. The Hf precursor employed was TEMAH, which was heated to 120 °C and delivered to the reactor chamber at 130 °C. H<sub>2</sub>S (3.5%, balance Ar) with a flow rate of 150 standard cubic centimeter per minute (sccm) was used as the S source. A remote plasma source operating at the power of 1000 W was used for the H<sub>2</sub>S plasma step. The deposition temperature was varied from 150 °C to 500 °C and the chamber pressure was controlled at 6 hundred Pa (hPa), regardless of the deposition temperature. Two precursors were alternately exposed to the substrates and subsequently purged for each precursor in an ALD cycle. One growth cycle consists of four main steps: (i) 1.6 s exposure to TEMAH, (ii) 10 s N<sub>2</sub> purge, (iii) 10 s exposure to H<sub>2</sub>S, (iv) 10 s N<sub>2</sub> purge. By repeating these steps, HfS<sub>2</sub> thin films with desired layers can be obtained. The possible reaction is as follows:



### 2.2. Characterization

The thickness of the HfS<sub>2</sub> films was measured by x-ray reflectivity using a PANalytical instrument. Atomic force microscope (AFM) was performed with tapping mode on a SPA400-Nanonavi instrument. Raman spectra were measured with 532 nm excitation under ambient conditions using ID-Spec ARCTIC, and the power levels on the sample were 0.1 mW. The x-ray diffraction (XRD) was performed on a Rigaku IV instrument. The x-ray photoelectron spectroscopy (XPS) was performed on a PHI Quantum-2000 instrument, and a conventional Al K $\alpha$  anode was used as the source of x-ray radiation.

## 3. Results and discussion

### 3.1. Self-limiting growth and thickness control

The self-limiting growth behavior of the ALD process for HfS<sub>2</sub> thin films was investigated at temperatures ranging

from 150 °C to 500 °C. Figure 1(a) shows the variation in the growth rate of HfS<sub>2</sub> films as a function of temperature. The HfS<sub>2</sub> film thickness was evaluated via x-ray reflectivity measurement. A saturated growth rate per cycle (GPC) of about 0.11 nm was estimated at temperatures ranging from 150 °C to 350 °C. When the growth temperature was higher than 450 °C, the growth rate started to surge from 0.17 nm to 0.8 nm per cycle at 500 °C. Therefore, the ALD temperature window between 150 °C and 350 °C for the growth of ALD-HfS<sub>2</sub> using TEMAH and remote H<sub>2</sub>S plasma was confirmed. Figure 1(b) shows the variation in the thickness of the HfS<sub>2</sub> films grown at 250 °C as a function of the number of cycles. Under basic pulsing conditions, the number of reaction cycles was varied from 80 to 500. The film thickness roughly linearly increases with the number of cycles, and the GPC is calculated to be 0.11 nm per cycle from the slope of the linear fit.

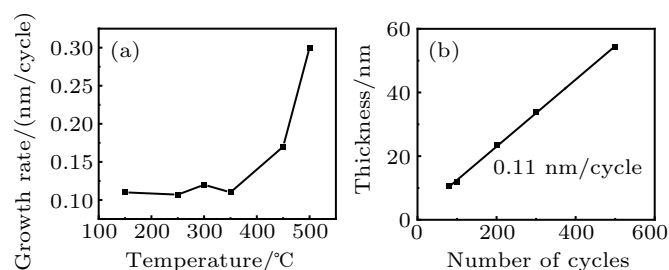


**Fig. 1.** (a) Variation in the growth rate of HfS<sub>2</sub> films as a function of temperature. (b) Variation in the thickness of HfS<sub>2</sub> films grown at 250 °C as a function of the number of cycles.

### 3.2. Surface morphology

The optical images of samples grown on 300 nm SiO<sub>2</sub>/Si, sapphire, and Si substrates by RPALD are shown in Fig. 2. At different growth temperatures, the surface colors of the HfS<sub>2</sub> films are uniform and slightly different, and they are all different from those of the bare substrates. Along with the increase of the growth temperature, the colors of the HfS<sub>2</sub> films on 300 nm SiO<sub>2</sub>/Si wafer (Figs. 2(a)–2(e)) uniformly change from dark yellow green to light yellow green, and then to dark yellow green again. For the HfS<sub>2</sub> films deposited on sapphire wafer (Figs. 2(f)–2(j)), the colors change from transparency to a slight tan. For the HfS<sub>2</sub> films deposited on Si wafer (Figs. 2(k)–2(o)), the colors also change to brown compared with the bare Si substrate. It is visibly clear that the deposited HfS<sub>2</sub> films are continuous and uniformly flat across the wafer.

We also examined the surface morphology of the HfS<sub>2</sub> films by AFM and SEM measurements. The AFM images of the as-grown HfS<sub>2</sub> films deposited on Si substrates for 100 cycles at various temperatures are shown in Figs. 3(a)–3(c). The surface of all HfS<sub>2</sub> films is uniform and smooth with similar surface morphology. The root-mean-square (RMS) surface roughness of the HfS<sub>2</sub> films slightly increases from 0.32 nm to 0.76 nm with increasing growth temperature from 250 °C to 450 °C. Figures 3(d)–3(f) show the SEM images of the HfS<sub>2</sub>

films deposited on Si for 100 cycles at 250 °C, 350 °C, and 450 °C, respectively. Small grains in the smooth surface are observed for all the HfS<sub>2</sub> films, indicating that the continuous and uniform HfS<sub>2</sub> films are deposited in the self-limiting growth window.

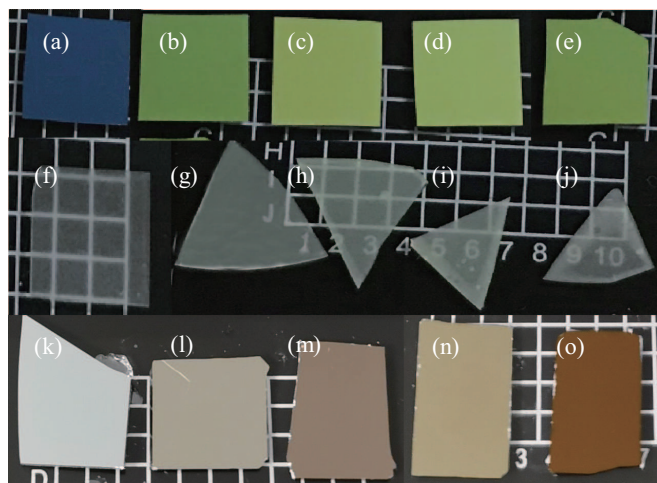


**Fig. 2.** Optical images of the HfS<sub>2</sub> films deposited for 300 cycles on 300 nm SiO<sub>2</sub>/Si, sapphire, and Si substrates. (a) Bare 300 nm SiO<sub>2</sub>/Si; HfS<sub>2</sub> films deposited on SiO<sub>2</sub>/Si at (b) 150 °C, (c) 250 °C, (d) 350 °C, (e) 450 °C; (f) bare sapphire; HfS<sub>2</sub> films deposited on sapphire at (g) 150 °C, (h) 250 °C, (i) 350 °C, (j) 450 °C; (k) bare Si; HfS<sub>2</sub> films deposited on Si at (l) 150 °C, (m) 250 °C, (n) 350 °C, (o) 450 °C.

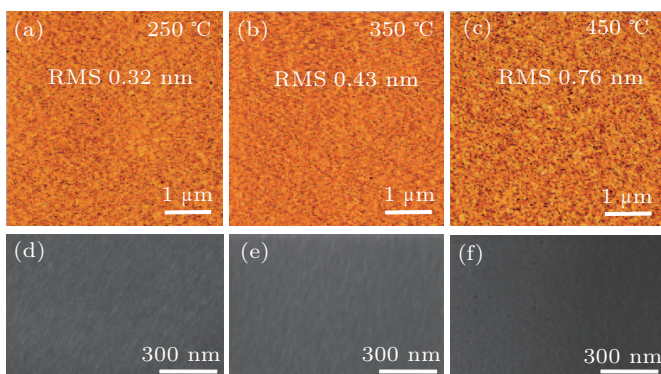


**Fig. 3.** AFM images of the HfS<sub>2</sub> films deposited on Si for 100 cycles at (a) 250 °C, (b) 350 °C, and (c) 450 °C. SEM images of the HfS<sub>2</sub> films deposited on Si for 100 cycles at (d) 250 °C, (e) 350 °C, and (f) 450 °C.

In order to study the effect of substrate on the surface morphology of the deposited HfS<sub>2</sub> films, the AFM images of the samples grown on Si and sapphire substrates are compared. Figures 4(a)–4(d) show the 500 nm×500 nm AFM images of the HfS<sub>2</sub> films deposited on Si and sapphire substrates at 450 °C for 80 cycles and 300 cycles, respectively. The surface of the HfS<sub>2</sub> films on both Si and sapphire substrates becomes rougher with the thickness increasing from 13.6 nm (80 cycles) to 51.0 nm (300 cycles), indicating that the grain size increases with HfS<sub>2</sub> thickness obviously. Figure 4(e) shows the grain size statistical distribution of the HfS<sub>2</sub> deposited for 80 cycles and 300 cycles on Si and sapphire. The grain size of HfS<sub>2</sub> is mainly distributed in 15–25 nm for 80 cycles and 20–30 nm for 300 cycles. The average grain size of HfS<sub>2</sub> increases from 22.3 nm to 27.1 nm for the samples deposited for

80 cycles and 300 cycles on Si, and from 22.2 nm to 24.1 nm for the samples on sapphire.

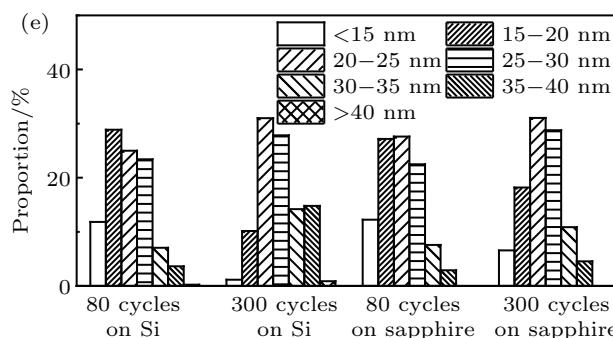
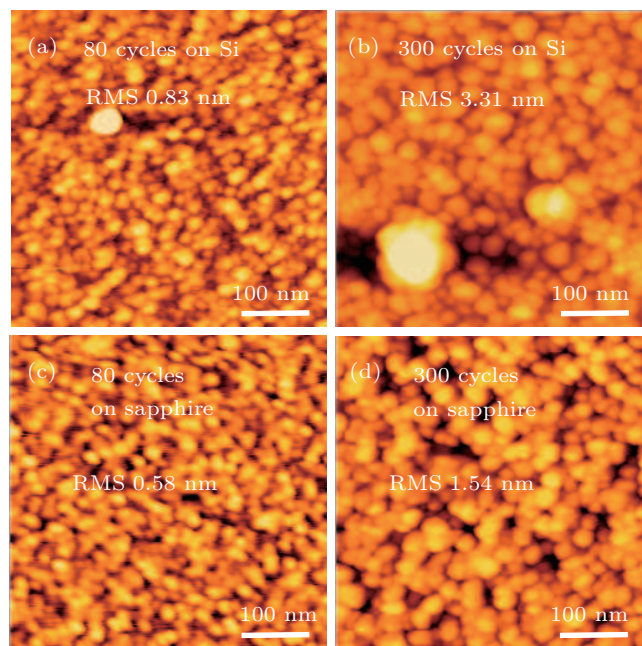


**Fig. 4.** AFM images of the HfS<sub>2</sub> films deposited at 450 °C for (a) 80 cycles on Si; (b) 300 cycles on Si; (c) 80 cycles on sapphire; (d) 300 cycles on sapphire. (e) Grain size statistical distribution of the HfS<sub>2</sub> deposited for 80 cycles and 300 cycles on Si and sapphire.

### 3.3. Chemical composition

Auger electron spectroscopy was used to analyze the element fraction in the HfS<sub>2</sub> thin films. Figure 5 shows the depth

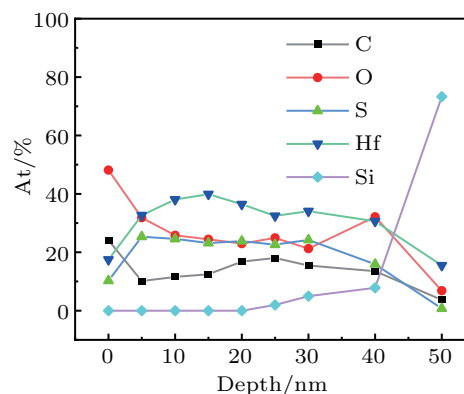


**Fig. 5.** Depth profile of elements in the HfS<sub>2</sub> film deposited on Si at temperature of 350 °C for 300 cycles.

profile of elements in the HfS<sub>2</sub> films deposited at 350 °C for 300 cycles. The oxygen content on the surface is much higher than that in the inside, suggesting that oxidation of HfS<sub>2</sub> easily occurs under ambient conditions. With the depth changing from 10 nm to 30 nm, the element contents of Hf, S, and O basically keep constant. The atomic percentages of Hf, O, and

S are about 35%, 25%, and 25%, respectively. It indicates that the deposited films under this condition have some HfO<sub>2</sub> mixing in HfS<sub>2</sub>. The content of Si starts increasing dramatically at the depth of 30 nm, indicating that the HfS<sub>2</sub> film thickness is about 30 nm, which is consistent with the deposited film thickness (33 nm) measured by x-ray reflectivity.

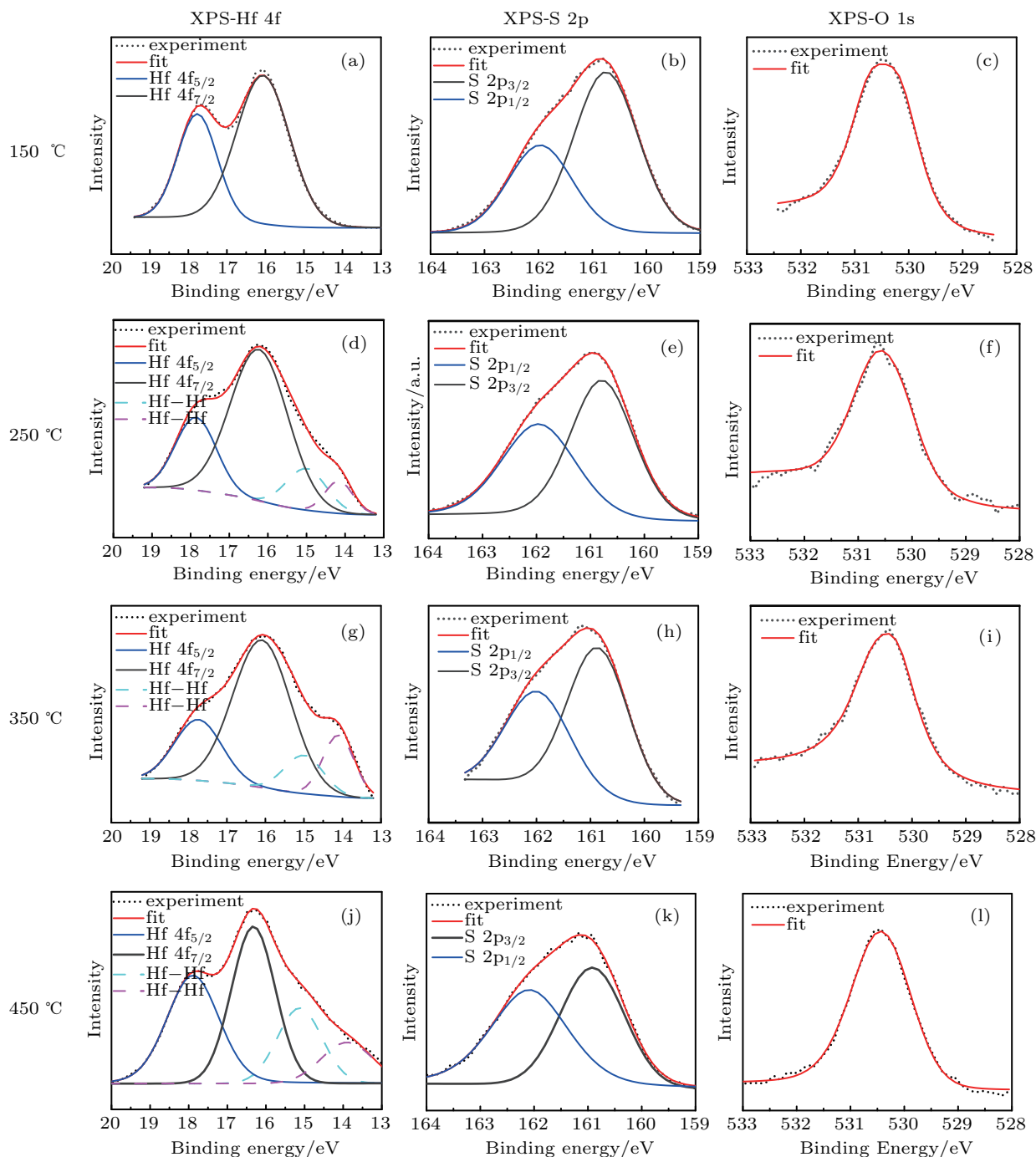


**Fig. 6.** XPS core-level spectra of the ALD-HfS<sub>2</sub> films prepared by 80 ALD cycles at (a)–(c) 150 °C, (d)–(f) 250 °C, (g)–(i) 350 °C, and (j)–(l) 450 °C: (a), (d), (g), (j) Hf 4f; (b), (e), (h), (k) S 2p; (c), (f), (i), (l) O 1s.

In order to further determine the chemical states of Hf, S, and O in the films, XPS was used to evaluate the formation of chemical bonding in the HfS<sub>2</sub> films. To remove oxidation of the surface, 5 nm HfS<sub>2</sub> films on the surface were etched away by Ar ions. The XPS spectra of the surface and

at 5 nm depth of the HfS<sub>2</sub> films were tested. Figure 6 shows the XPS spectra at 5 nm depth of the HfS<sub>2</sub> films grown for 80 cycles at 150 °C, 250 °C, 350 °C, and 450 °C, respectively. For the XPS spectra of the HfS<sub>2</sub> film deposited at 150 °C, Hf 4f<sub>7/2</sub> and Hf 4f<sub>5/2</sub> components are found at 16.1 eV and

17.8 eV (Fig. 6(a)), respectively. A broad feature appears in the S 2p region with  $2p_{3/2}$  and  $2p_{1/2}$  components at 160.9 eV and 162.1 eV (Fig. 6(b)), respectively. These features are consistent with the  $\text{HfS}_2$  peak positions reported previously.<sup>[10,11]</sup> The O 1s peaks at 530.4 eV binding energy are associated with  $\text{HfO}_2$ ,<sup>[27]</sup> as shown in Fig. 6(c). However, compared with that of Hf 4f bonding to S, the spectra of Hf–O bond (near 19.1 eV)<sup>[10]</sup> is too small to be detected. For the XPS spectra of the  $\text{HfS}_2$  film deposited at 250 °C, in addition to the Hf–S spectra, the peaks at 14.1 eV and 15.2 eV (Fig. 6(d)) binding

energy are attributed to the Hf–Hf bond,<sup>[35]</sup> which are introduced by the Ar ion etching process. Figure 6(e) shows the binding energy of S 2p bonding to S, and figure 6(f) shows the binding energy of O 1s bonding to Hf. Similarly, the XPS spectra of the  $\text{HfS}_2$  films grown at 350 °C (Figs. 6(g)–6(i)) and 450 °C (Figs. 6(j)–6(l)) show the same characteristics as those grown at 250 °C. The full XPS spectra demonstrate that the as-grown  $\text{HfS}_2$  films are of correct chemical composition but mixed with  $\text{HfO}_2$ .

**Table 1.** Atomic percentages of Hf, S, and O in  $\text{HfS}_2$  thin films evaluated by the sensitivity factor method from XPS.

Deposition temperature	Surface			Etching 5 nm		
	Hf/%	S/%	O/%	Hf/%	S/%	O/%
150 °C	21.211	25.816	52.974	22.765	51.890	25.345
250 °C	18.869	36.817	44.314	20.389	70.512	09.100
350 °C	20.139	42.732	37.129	24.673	54.622	20.705
450 °C	27.680	19.175	53.146	31.243	25.400	43.357

According to the XPS measurement of the surface and at 5 nm depth of the  $\text{HfS}_2$  films, the atomic percentages of Hf, S, and O in the  $\text{HfS}_2$  thin films were evaluated by the sensitivity factor method, and the results are listed in Table 1. The Hf content is approximately 25% and the element contents of S and O in total are around 75%, suggesting the mixture of  $\text{HfO}_2$  and  $\text{HfS}_2$ . The element content of S at 5 nm depth of the  $\text{HfS}_2$  films is higher than that at the surface, while the element content of O at the surface of the  $\text{HfS}_2$  films is much higher than that at 5 nm depth. These results suggest that the as-deposited  $\text{HfS}_2$  is easily oxidized in the atmosphere. The S content in the films deposited at less than 450 °C is much higher than the O content, indicating that  $\text{HfS}_2$  is the dominant component in the films. Almost pure  $\text{HfS}_2$  films can be obtained at 250 °C. When the deposition temperature is as high as 450 °C, the  $\text{HfS}_2$  films become oxygen-rich. Oxygen incorporation mechanism and suppression need further investigation.

### 3.4. Film crystallinity

Raman spectra of the  $\text{HfS}_2$  films grown on  $\text{SiO}_2/\text{Si}$  for 300 cycles at various temperatures are shown in Fig. 7(a). Besides the peaks from the Si substrate ( $300\text{ cm}^{-1}$ ), there are only two peaks located at  $260\text{ cm}^{-1}$  and  $338\text{ cm}^{-1}$ , corresponding to the in-plane vibrational mode ( $E_{2g}^1$ ) and out-plane vibrational mode ( $A_{1g}$ ) of  $\text{HfS}_2$ , respectively. Strong Raman peaks from the  $\text{HfS}_2$  films deposited at the temperatures from 250 °C to 450 °C show the formation of a locally ordered structure. The lack of Raman peaks of both  $E_{2g}^1$  and  $A_{1g}$  modes for the  $\text{HfS}_2$  films deposited at 150 °C suggests that the  $\text{HfS}_2$  films are amorphous. Combined with the observation of grains in the SEM and AFM images, it is demonstrated that nanocrystal  $\text{HfS}_2$  films are achieved with RPALD at lower temperature down to 250 °C. The grain size of  $\text{HfS}_2$  increases with the

increase of the thickness and growth temperature. Higher deposition temperature improves the atomic ordering in the  $\text{HfS}_2$  films, resulting in significant improvement of intensities of the characteristic  $E_{2g}^1$  and  $A_{1g}$  modes.

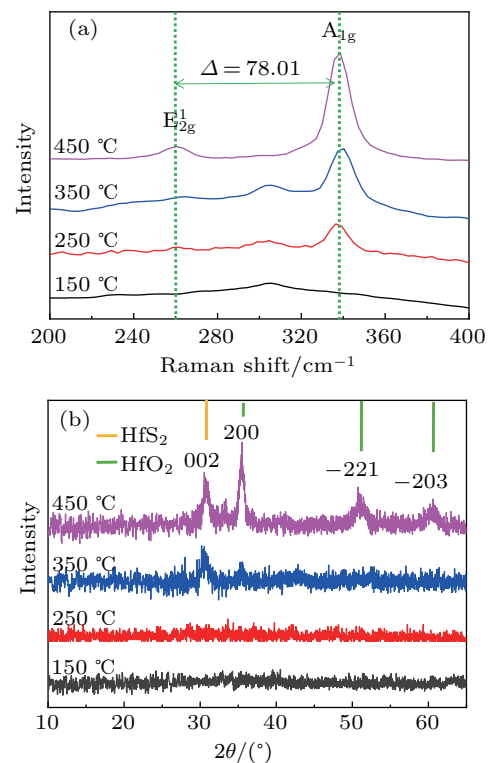


**Fig. 7.** Film crystallinity of  $\text{HfS}_2$  films deposited for 300 cycles. (a) Raman spectra of  $\text{HfS}_2$  films deposited at 150–450 °C. (b) GIXRD patterns of  $\text{HfS}_2$  films deposited at 150–450 °C.

Grazing incident XRD was also used to study the structural properties and crystalline nature of the  $\text{HfS}_2$  films. Grazing incident XRD patterns of the as-grown  $\text{HfS}_2$  films with small signal from the oxide phase are shown in Fig. 7(b). There are no diffraction peaks observed for the films deposited

at 150 °C and 250 °C. As the growth temperature increases, HfS<sub>2</sub> films deposited at 350 °C show a crystalline HfS<sub>2</sub> (002) diffraction peak at 30.5° and a weak HfO<sub>2</sub> (200) diffraction peak at 35.6° in the XRD pattern. When the growth temperature increases to 450 °C, besides the enhanced HfS<sub>2</sub> (002) and HfO<sub>2</sub> (200) peaks, two new diffraction peaks appear at 50.8° and 60.4°, corresponding to HfO<sub>2</sub> (−221) and HfO<sub>2</sub> (−203) diffraction peaks, respectively. These results show that the crystallinity of HfS<sub>2</sub> is improved with the increase of the deposition temperature. However, a temperature as higher as 450 °C could also cause the transformation of nanocrystal HfO<sub>2</sub> mixed in the HfS<sub>2</sub> to polycrystalline.

#### 4. Conclusions

In summary, we have successfully deposited HfS<sub>2</sub> nanocrystal thin films by RPALD at low temperature with TEMAH and H<sub>2</sub>S as the precursors. Self-limiting growth behavior is observed in the temperature range of 150 °C to 350 °C with a growth rate of about 0.11 nm/cycle. The surface of the deposited HfS<sub>2</sub> is smooth with the appearance of uniformly nanocrystal grains. The size of the nanocrystal grain depends on the growth temperature, the kind of substrate, and the HfS<sub>2</sub> film thickness. The crystalline HfS<sub>2</sub> is achieved at lower temperature down to 250 °C, and the crystal quality is significantly improved with increasing deposition temperature. However, the as-deposited HfS<sub>2</sub> films are almost oxygen-rich, in which crystallized HfO<sub>2</sub> is detected for the sample deposited at higher temperature. In addition, the as-deposited HfS<sub>2</sub> is easily oxidized in the atmosphere. Further investigation is needed to lower the oxygen content and increase the crystallinity of the HfS<sub>2</sub> films. Low temperature atomic layer deposition is believed to be a promising route to large area HfS<sub>2</sub> nanocrystal thin films growth for electronic or electrochemical applications in the future.

#### References

- [1] Butler S Z, Hollen S M, Cao L, Cui Y, Gupta J A, Gutiérrez H R, Heinz T F, Hong S S, Huang J, Ismach A F, Johnston-Halperin E, Kuno M, Plashnitsa V V, Robinson R D, Ruoff R S, Salahuddin S, Shan J, Shi L, Spencer M G, Terrones M, Windl W and Goldberger J E 2013 *ACS Nano* **7** 2898
- [2] Wang Q H, Kalantar-Zadeh K, Kis A, Coleman J N and Strano M S 2012 *Nat. Nanotechnol.* **7** 699
- [3] Manzeli S, Ovchinnikov D, Pasquier D, Yazyev O V and Kis A 2017 *Nat. Rev. Mater.* **2** 17033
- [4] Choi W, Choudhary N, Han G H, Park J, Akinwande D and Lee Y H 2017 *Mater. Today* **20** 116
- [5] Duong D L, Yun S J and Lee Y H 2017 *ACS Nano* **11** 11803
- [6] Kanazawa T, Amemiya T, Ishikawa A, Upadhyaya V, Tsuruta K, Tanaka T and Miyamoto Y 2016 *Sci. Rep.* **6** 22277
- [7] Mirabelli G, McGeough C, Schmidt M, McCarthy E K, Monaghan S, Povey I M, McCarthy M, Gity F, Nagle R, Hughes G, Cafolla A, Hurley P K and Duffy R 2016 *J. Appl. Phys.* **120** 125102
- [8] Chae S H, Jin Y, Kim T S, Chung D S, Na H, Nam H, Kim H, Perello D J, Jeong H Y, Ly T H and Lee Y H 2016 *ACS Nano* **10** 1309
- [9] Wang D, Zhang X and Wang Z 2018 *J. Nanosci. Nanotechnol.* **18** 7319
- [10] Yan C, Gan L, Zhou X, Guo J, Huang W, Huang J, Jin B, Xiong J, Zhai T and Li Y 2017 *Adv. Funct. Mater.* **27** 1702918
- [11] Wang D, Zhang X, Liu H, Meng J, Xia J, Yin Z, Wang Y, You J and Meng X M 2017 *2D Mater.* **4** 031012
- [12] Fu L, Wang F, Wu B, Wu N, Huang W, Wang H, Jin C, Zhuang L, He J, Fu L and Liu Y 2017 *Adv. Mater.* **29** 1700439
- [13] Kaur H, Yadav S, Srivastava A K, Singh N, Rath S, Schneider J J, Sinha O P and Srivastava R 2018 *Nano Res.* **11** 343
- [14] Zheng B, Chen Y, Wang Z, Qi F, Huang Z, Hao X, Li P, Zhang W and Li Y 2016 *2D Mater.* **3** 035024
- [15] Wang D, Meng J, Zhang X, Guo G, Yin Z, Liu H, Cheng L, Gao M, You J and Wang R 2018 *Chem. Mater.* **30** 3819
- [16] Zheng B, Wang Z, Qi F, Wang X, Yu B, Zhang W and Chen Y 2018 *Appl. Surf. Sci.* **435** 563
- [17] Brooks D J, Douthwaite R E, Brydson R, Calvert C, Measures M G and Watson A 2006 *Nanotechnology* **17** 1245
- [18] Oh S, Kim J B, Song J T, Oh J and Kim S H 2017 *J. Mater. Chem. A* **5** 3304
- [19] Huang Y, Liu L and Liu X 2019 *Nanotechnology* **30** 95402
- [20] Nandi D K, Sen U K, Choudhury D, Mitra S and Sarkar S K 2014 *Electrochim. Acta* **146** 706
- [21] Jin Z, Shin S, Kwon D H, Han S J and Min Y S 2014 *Nanoscale* **6** 14453
- [22] Kwon D H, Jin Z, Shin S, Lee W S and Min Y S 2016 *Nanoscale* **8** 7180
- [23] Xiong D, Zhang Q, Li W, Li J, Fu X, Cerqueira M F, Alpuim P and Liu L 2017 *Nanoscale* **9** 2711
- [24] Kim H J, Jeon H and Shin Y H 2018 *J. Appl. Phys.* **124** 115301
- [25] Shimizu J, Ohashi T, Matsuura K, Muneta I, Kuniyuki K, Tsutsui K, Ikarashi N and Wakabayashi H 2019 *IEEE J. Electron. Devices Soc.* **7** 76
- [26] Hao W, Marichy C and Journet C 2019 *2D Mater.* **6** 012001
- [27] Groven B, Mehta A N, Bender H, Smets Q, Meersschaert J, Franquet A, Conard T, Nuytten T, Verdonck P, Vandervorst W, Heyns M, Radu I, Caymax M and Delabie A 2018 *J. Vac. Sci. Technol. A Vac. Surf. Film* **36** 01A105
- [28] Wu Y, Raza M H, Chen Y C, Amsalem P, Wahl S, Skrodzky K, Xu X, Lokare K S, Zhukush M, Gaval P, Koch N, Quadrelli E A and Pinna N 2019 *Chem. Mater.* **31** 1881
- [29] Yeo S, Nandi D K, Rahul R, Kim T H, Shong B, Jang Y, Bae J S, Han J W, Kim S H and Kim H 2018 *Appl. Surf. Sci.* **459** 596
- [30] Pyeon J J, Baek I H, Lim W C, Chae K H, Han S H, Lee G Y, Baek S H, Kim J S, Choi J W, Chung T M, Han J H, Kang C Y and Kim S K 2018 *Nanoscale* **10** 17712
- [31] Lee N, Lee G, Choi H, Park H, Choi Y, Kim K, Choi Y, Kim J W, Yuk H, Sul O, Lee S B and Jeon H 2019 *Appl. Surf. Sci.* **496** 143689
- [32] Lv J and Liu L 2020 *Nanotechnology* **31** 055602
- [33] Hämäläinen J, Mattinen M, Mizohata K, Meinander K, Vehkamäki M, Räisänen J, Ritala M and Leskelä M 2018 *Adv. Mater.* **30** 1703622
- [34] Mattinen M, Popov G, Vehkamäki M, King P J, Mizohata K, Jalkanen P, Räisänen J, Leskelä M and Ritala M 2019 *Chem. Mater.* **31** 5713
- [35] Chi X, Lan X, Lu C, Hong H, Li C, Chen S, Lai H, Huang W and Xu J 2016 *Mater. Res. Express* **3** 035012